frontiers | Frontiers in Materials

TYPE Original Research
PUBLISHED 05 January 2023
DOI 10.3389/fmats.2022.1052870

OPEN ACCESS

EDITED BY
Valter Carvelli,
Politecnico di Milano, Italy

REVIEWED BY
Peng Zhang,
Qingdao University of Technology, China
Maurizio Guadagnini,
The University of Sheffield,
United Kingdom

*CORRESPONDENCE
Zakaria Che Muda,
zakaria.chemuda@newinti.edu.my
Mudthir Bakri,
m.almakkki@qu.edu.sa

SPECIALTY SECTION
This article was submitted to Structural Materials,
a section of the journal
Frontiers in Materials

RECEIVED 24 September 2022
ACCEPTED 19 December 2022
PUBLISHED 05 January 2023

CITATION
Abusogi MA, Muda ZC, Hafez MA and Bakri M (2023), Effect of polypropylene fibre on cementitious mortar early shrinkage cracking using the eccentric-ring test.
Front. Mater. 9:1052870.
doi: 10.3389/fmats.2022.1052870

Effect of polypropylene fibre on cementitious mortar early shrinkage cracking using the eccentric-ring test

Maha A. Abusogi[1], Zakaria Che Muda[1]*, Mohamed Ahmed Hafez[1] and Mudthir Bakri[2]*

[1]Department of Civil Engineering, Faculty of Engineering and Quantity Surveying, INTI International University, Nilai, Malaysia, [2]Department of Civil Engineering, College of Engineering, Qassim University, Unaizah, Saudi Arabia

The effects of polypropylene fibres on mortar and cement-paste cracking were investigated using different amounts of fibre fractions and eccentric rings under restrained-shrinkage conditions. Eccentric-ring tests were conducted to investigate early-age shrinkage cracks. The characteristics of restricted cementitious materials were described by evaluating the cracking time and using concrete mixtures that are less likely to crack. Different fibre-volume fractions significantly enhanced the width, area, and age of cracking. Increasing the water-cement ratio and sand percentage increased the cracking age. The eccentric-ring test showed a greater susceptibility to cracking in cement-mortar composites. The mechanical strength was assessed, and the impact of polypropylene fibres was investigated.

KEYWORDS

early-age shrinkage cracking, polypropylene fibres (PP), eccentric ring test, crack width, cementitious mortar

1 Introduction

In the concrete industry, cracking of cementitious products presents a serious challenge. The formation of cracks significantly affects not only the mechanical qualities of concrete but also its durability. Rapid penetration of harsh chemicals, enhanced carbonation, and faster corrosion of reinforcement in concrete are indicators of decreased durability. Under certain circumstances, shrinkages of cement-based materials cause internal stress during the initial stages of hydration, and may lead to cracking if the strain is not dispersed (Wongtanakitcharoen and Naaman, 2007; Choktaweekarn and Tangtermsirikul, 2009; Kanavaris et al., 2019; Idrees et al., 2022).

The American Society for Testing and Materials (ASTM) and American Association of State Highway and Transportation Officials (AASHTO) recommended confined ring tests to assess the probability of early-age cracking in mortar and other cementitious materials. However, the concentric ring test has drawbacks in that fractures and cracks appear at random locations. Additionally, the cracking duration of a specimen is significantly prolonged (Dong et al., 2014; Zhou et al., 2014; Dong et al., 2017; Kanavaris et al., 2019). New ring test techniques, such as the elliptical ring test (Dong et al., 2014; Dong et al., 2017; Dong et al., 2018) and square-eccentric-ring test (Branston et al., 2016), have been suggested as a substitute for the circular ring-test method for decreasing the ring-test time and observing the crack growth.

Reinforcing concrete with fibres significantly improves the mechanical properties, enhancing the ductility, while providing more dynamic stress resistance. Furthermore, it is

a highly effective method for controlling and reducing the development of drying-shrinkage cracking (Abusogi and Bakri, 2022; Zhang et al., 2022). This method also controls and reduces the likelihood of cracks appearing because of drying shrinkage. Using fibres as a secondary reinforcing mechanism releases the tension formed during drying. It has the potential to prevent crack propagation and scabbing failures (Wongtanakitcharoen and Naaman, 2007; Banthia and Gupta, 2006; Juarez et al., 2015). It is of utmost importance to be aware of the circumstances in which a particular kind of fibre performs at its peak, as well as the volume fraction (V_f) that might minimise the overall drying shrinkage (Alavi Nia et al., 2012; Sadiqul Islam and Gupta, 2016; Saradar et al., 2018).

Polypropylene (PP) fibres are the most efficient and cost-effective type of fibres available today for concrete (Tang et al., 2018). They are also believed to be inert in high-pH cementitious environments. They are simple to disperse in cement mortar and concrete mixes. However, the precise impact of the PP fibre shape, diameter, length, fibrillations, and other factors is not completely known. Different approaches may be used to investigate the shrinkage-induced cracking in cement-based materials. The two specimens used most often are the ring-type and linear specimens with fastened ends (Banthia et al., 1993; Yousefieh et al., 2017).

The findings of previous tests show that using PP fibres may significantly reduce the drying and overall shrinkage of concrete. Some studies (Juarez et al., 2015) have examined how employing various fibres with different aspect ratios affects the cracking characteristics.

Previous research found that adding a .2% V_f of 15 mm long PP fibre to alkali-activated slag mortar minimised drying shrinkage by 37.1%. This was achieved by adding PP fibres. In addition, there has been evidence of good bonding between the matrix and PP fibres, which is directly proportional to the enhancement of the material's mechanical characteristics (Xu et al., 2021).

The results of a previous study (Wu et al., 2020; Rani et al., 2022) indicate that the PP fibre enhances the performance of concrete by preventing chloride penetration and extends its lifespan. The findings also show that adding PP fibres to concrete increases the resilience of the material to high-temperature exposure.

According to the findings, including fibre in the mix boosts compressive strength by 16%, 20%, and 3% at ages 3, 7, and 28 days, respectively. Additionally, it enhanced the flexural toughness index by up to 7.7 times. Further, fractures formed to their maximum depth in every single one of the concrete ring tests, except for the combination that included PP. The combination of PP fibres reduces the effect of reducing crack width by up to 62% while simultaneously enhancing age cracking by up to 84% (Saradar et al., 2018) Further, adding fibres at a relatively high volume percentage of 5% improved the compressive strength and flexural toughness of mortar specimens (McLain, 1974; Boghossian and Wegner, 2008).

An eccentric-ring geometry was used to determine the degree of early-age shrinkage cracking under restrained conditions. The initial cracking was predicted to occur earlier than that in a circular geometry to reduce the experiment duration. It was previously proven that an eccentric ring has a higher stress intensity owing to the geometrical effect (Hossain and Weiss, 2006; Dong et al., 2014).

The use of eccentric rings was proposed as a different experimental approach to detect the potential of cement-based composite cracking under hight restraint conditions and to achieve a quicker and more accurate evaluation of the cracking tendency of cementitious composites (Abusogi and Wei, 2018; Tian and Wei, 2019). The most significant distinction is that the cementitious material in the eccentric rings is placed under complex and non-uniform circumferential stress owing to the eccentricity between the outer and inner circles. The cracks in the restrained cementitious rings started at the internal circumference and progressed to the outside circumference towards the arrow side. The cracks subsequently move and propagate across the ring wall, depending on the amount of water in the cement.

To explore the mechanism of this test method in detail, previous studies utilised numerical analysis to simulate stress development and crack initiation in cementitious ring specimens under restrained-shrinkage, considering the coupling of thermal, moisture diffusion, and mechanical analyses (Abusogi and Wei, 2018; Abusogi and Wei, 2019). Thermal characteristics were used to calculate the nodal temperature. Moisture diffusion was investigated by considering the relationship between the differential equation that regularises the heat-transfer analysis and moisture diffusion. Previous research has shown the relevance of employing an eccentric-ring mould to analyse early-age shrinkage cracking (Abusogi et al., 2017; Abusogi and Bakri, 2022).

The purpose of this study was to evaluate the characteristics of restraint-drying shrinkage and mechanical strength of cementitious mortar reinforced with PP fibres at w/c ratios of .3, .4, and .5, with three different fibre V_f values of .4%, .6%, and .8%. To achieve this goal, the restraint-drying shrinkage was measured using an eccentric-ring test. The early-age cracks were assessed in the presence of a more complicated and non-uniform circumferential stress, and the effect of PP fibres was examined. The properties of drying-shrinkage cracks (crack width, age, and area) were investigated. The compressive and tensile strengths of the cement paste and mortar with fibres were examined. Finally, two variables were chosen (W/C ratio and volume fraction) as input parameters for the analysis of early-age cracking, crack width, compressive strength, and tensile strength of the cement paste and mortar with fibres. All tests were completed in an environmental test room at a temperature of 20°C and a relative humidity of 45%. All specimens were kept for 24 h in a curing room at a temperature of 20°C and a humidity of 98%, to achieve a standardised evaporation rate.

2 Materials and methods

2.1 Materials

2.1.1 Cement

All mixing in this investigation was completed using Type 1 ordinary Portland cement (OPC) of a specific gravity of 3,153 kg/m^3 and a specific surface area of 3.19 m^2/g. Table 1 provides a summary of the OPC chemical components. The OPC chemical composition and fineness effect shrinking (Branston et al., 2016).

2.1.2 Mixing water and superplasticisers (SP)

Potable water free from contaminants or impurities from a municipal tap was used for mixing and curing. High-performance solid superplasticiser type β-naphthalene and ranged from .1, .2, and .25% of cement weight with a fibre V_f of .4%, .6%, and .8% and w/c of .3 to achieve more workable enhance the workability of the fresh mortar.

TABLE 1 Chemical composition of the used ordinary Portland cement (OPC).

Composition	CaO	SiO_2	Al_2O_3	Fe_2O_3	MgO	Na_2O	K_2O	SO_3
Mass fraction (%)	65.22	19.28	5.88	3.46	1.16	0.1	.12	1.87

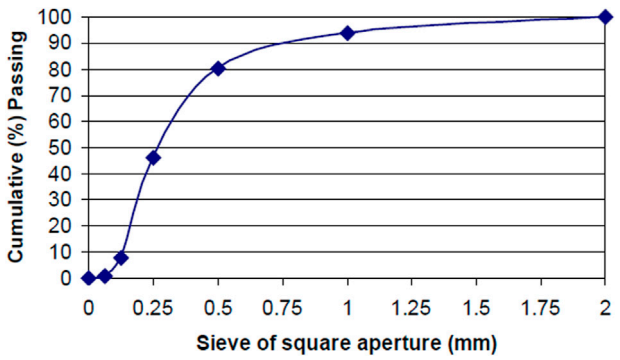

FIGURE 1
Cumulative (%) passing of sand particle.

FIGURE 2
Type of PP fibre sample used.

2.1.3 Fine aggregate (sand)

Sieve analysis was performed according to the Chinese Standard (Zhang et al., 2006) to attain the particle size distribution of the fine aggregates utilised in this investigation, as shown in Figure 1. The sand was taken from local river sand. To get rid of any moisture that had been absorbed prior to material processing, the sand was pre-treated for 24 h in a drying oven at 105°C. Then particle size distribution was performed, confirming that the fineness modulus was three.

2.1.4 Monofilament PP fibres

The synthetic monofilament PP fibre shown in Figure 2 was derived from monomeric hydrocarbons of a specific gravity of 910 kg/m^3.

The good mechanical properties of PP fibres offer a fracture strength greater than 400 MPa and Young's modulus of 3.5 GPa. The mode of polymerisation gives PP a sterically regular atomic arrangement that results in its chemical inertness. Hence, it can be added to a highly alkaline matrix without any adverse effects on its properties. In this study, monofilament PP straight was proposed and added to cement mortar. Table 2 lists the characteristics of the PP fibres.

2.1.5 Mixing procedure

In the mixing procedure, fine aggregates, including PP fibres, were carefully incorporated during the mixing process in a cement rotary mixer at 45 rpm for 3–4 min, after that a further 3 min were spent mixing the cement in the mixer. The remaining mixing water and Superplasticisers were then incorporated into the mixture and mixed for another 5 min before pouring into ring-shaped moulds. The specimens were covered with lids to obtain a sealed off environment that prevented evaporation.

2.2 Design of the mix

Table 3 shows the amounts of each type of mix used in this study, as well as a description of the mix that was used. The proportion of cement remained constant at 1,200 kg/m^3 in all mixes. However, the sand, w/c ratio, and superplasticiser were varied based on the required mix design. The V_f of PP fibres varied from 0, .4%, .6%, and .8% based on the required mix design for the cement mortar and cement paste. For convenience, a mix code was assigned to each mix.

To obtain findings that were similar to those of other researchers who used various fibres, cement-to-sand ratios of 1:2 and 1:1 were used (Lye et al., 2022). To obtain insight into the advantages of the fibre in a more practical situation, where it is probable that their impact on workability will need to be taken into consideration using a superplasticiser and a mix with a low w/c ratio of .3 was selected. As a result, the superplasticiser dosage in the above table refers to the higher dosage necessary to provide an equal flow for raising the dosage of the fibre. Using a w/c ratio of .40, a high flow mixture was developed. This mixture is useful for testing in the lab because it causes considerable shrinkage and cracking, which makes it easier to see how the fibres work. Tables 4, 5 present the proportions of each mix used in this investigation for the mortar and cement-paste mixes, respectively.

In this study, three specimen mixtures with different w/c ratios were evaluated. Each mixture had a different fibre V_f of .4%, .6%, and .8%. The mix codes are labelled according to V_f (.4%, .6%, and .8%) in percentage and mixture composite with mortar (M1, M2, and M3) and cement paste (M4, M5, and M6) with different w/c ratios. PM1, PM2, and PM3 are the plain mortar control mixes. PM4, PM5, and PM6 are

TABLE 2 Geometry and mechanical characteristics of monofilament PP fibre.

PP monofilament fibre	Length (mm)	Diameter (μm)	Unit weight (g/cm^3)	Modulus of elasticity (GPa)	Fracture strength (MPa)
	20	100 ± 50	.91	>3.5	≥400

TABLE 3 Mass proportions of mixes used.

Mix code	OPC content (kg/m^3)	Sand (kg/m^3)	Water (kg/m^3)	Superplasticiser	Description
M1 (w/c = .3)	1,200	1,200	360	Varied	Cement-to-sand 1:1
M2 (w/c = .4)	1,200	2,400	480	—	Cement-to-sand 1:2
M3 (w/c = .5)	1,200	2,400	600	—	Cement-to-sand 1:2
M4 (w/c = .3)	1,200	0	360	Varied	Cement-paste material
M5 (w/c = .4)	1,200	0	480	—	Cement-paste material
M6 (w/c = .5)	1,200	0	600	—	Cement-paste material

TABLE 4 Fibre V_f (%) for mortar mixes.

Mix code	Fibre type	V_f (%)
PM1	—	0
M1-V_f .4		.4
M1-V_f .6	PP	.6
M1-V_f .8		.8
PM2	—	0
M2-V_f .4		.4
M2-V_f .6	PP	.6
M2-V_f .8		.8
PM3	—	0
M3-V_f .4		.4
M3-V_f .6	PP	.6
M3-V_f .8		.8

TABLE 5 Fibre V_f (%) for cement paste.

Mix code	Fibre type	V_f (%)
PM 4	—	.0
M4-V_f .4		.4
M4-V_f .6	PP	.6
M4-V_f .8		.8
PM5	—	.0
M5-V_f .4		.4
M5-V_f .6	PP	.6
M5-V_f .8		.8
PM6	—	.0
M6-V_f .4		.4
M6-V_f .6	PP	.6
M6-V_f .8		.8

the plain cement-paste control mixes with different w/c ratios without any fibre.

2.3 Experimental procedure

The specimens were cured according to ASTM standard C192. The samples were stored in a curing chamber for 24 h at 20°C and 98% humidity to maintain a standard rate of evaporation. All tests were conducted in an environmental test chamber at a temperature of 20°C and a relative humidity of 45%.

2.3.1 Mechanical-strength test

According to ASTMC1609, a tensile-strength test was performed on prismatic samples with dimensions of 160 mm × 40 mm × 40 mm. As reported in previous studies, the tests were conducted using a three-point MTS loading system with a loading rate of 50 N/s (Dalvand and Ahmadi, 2021; Abusogi and Bakri, 2022). The compressive strength was measured to investigate the strength development with respect to age. The samples were prepared, blended, and placed into a 40 mm^3 × 40 mm^3 × 40 mm^3 mould for a compressive-strength test based on the ASTM C109 standard. A hydraulically powered material-testing system (MT810) with a loading rate of 24 kN/s (C109/C109M-16a, 2016) was used. The samples were poured and cured until their test age was attained.

2.3.2 Restrained-shrinkage test

An experiment on the early-age drying shrinkage was conducted using the eccentric-ring test, as shown in Figure 3. The purpose was to provide a new method for measuring early crack development when subjected to a more complicated and non-uniform circumferential stress in eccentric-cementitious-composite rings (Abusogi and Wei, 2019; Tian and Wei, 2019). The samples exhibited yield crack propagation owing to restraint and changes in humidity arising

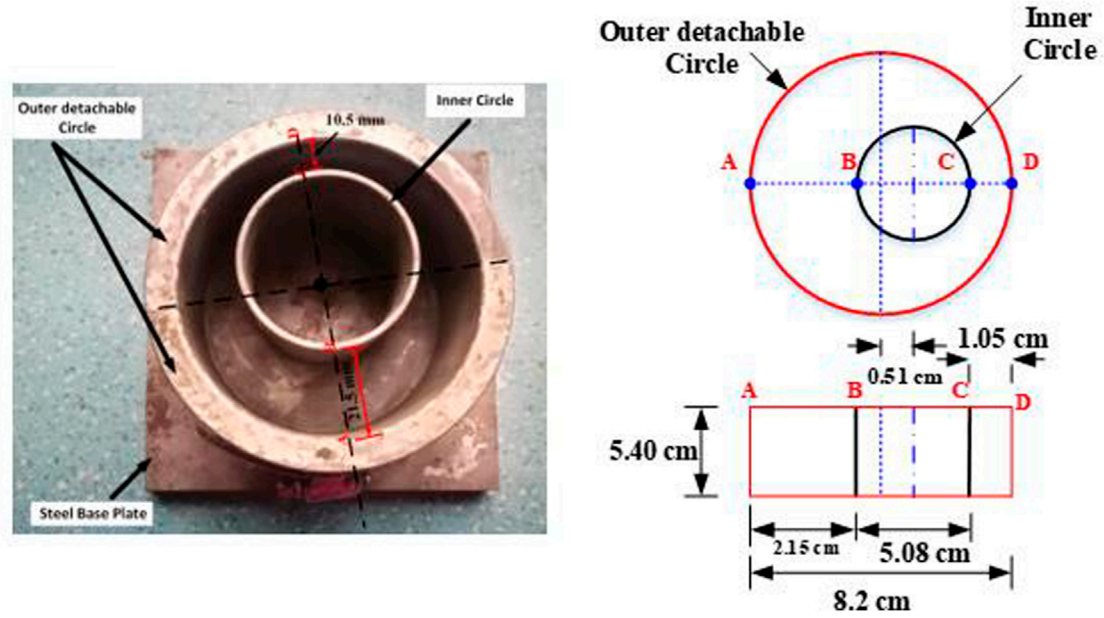

FIGURE 3
Eccentric restrained-shrinkage cracking frame.

from self-desiccation. To study the effect of geometry, a sample of cementitious composites was cast with the outer circumference of the inner eccentric steel core. Recent studies have focused on using mortar and cement paste as the material for restraint specimens and adding different dosages of fibres (V_f ratio). In this study, mortar was used to increase the magnitude of shrinkage strain and cracking severity such that the influence of the fibre can be more readily measured. The proportions of each type of mix used in this study, along with a description of the purpose of the mixes, are listed in Table 3.

The crack growth was slow and steady, as observed under a magnifying microscope. The crack age was recorded once it appeared on the surface of each specimen, and the largest crack width was recorded. The restrained-shrinkage test results are the computed mean values based on three specimens per recommended fibre dosage and w/c ratio.

As a result, current research has concentrated on employing mortar as the material for restraint specimens and varying the doses of fibres in relation to the V_f ratio. In this investigation, the size of the shrinkage strain and cracking severity were increased using mortar. Consequently, the impact of fibre could be measured more easily. Table 3 shows the amounts of each mix employed in this study, as well as an explanation of the mix functions. Under a magnification microscope, the fracture propagation was gradual and constant. When a crack manifested on the surface of each specimen, its age and the maximum width of the crack was immediately recorded. In this study, the results of the restricted shrinkage test are provided as the mean values computed from three specimens per suggested fibre dosage and w/c ratio.

2.4 Analysis method

To analyse the effect of the fibre-volume fraction (V_f) percentage and water-cement ratio on the relevant properties of mortar, the distance-weighted–least-squares approach was used to fit a curve to the data using the following process. Polynomial (second-order) regression was used to discover the matching Y value for each value on the X variable scale (McLain, 1974). This was performed such that the weight of each data point decreased as it moved away from the specific X value. McLain (1974) described an algorithm similar to the one used in this procedure (Rezaie et al., 2022). Multilinear regression was used to formulate the response of the tensile strength and crack width to changes in the amount of water to cement (w/c) and PP fibres [V_f (%)]. Multiple regression is an extension of ordinary least-squares (OLS) regression (Dahish et al., 2021), and uses more than one variable to describe the tensile strength and crack width in fibrous cementitious mortar.

The determination coefficient (R^2) was used to evaluate the accuracy of the prediction equations, as stated in the formula below:

$$R^2 = 1 - \frac{\sum_{i=1}^{N}(X - Y)^2}{\sum_{i=1}^{N} Y^2}$$

where X = measured from experiment and Y = multiple regression prediction.

This measure is given as a value between .0 and 1.0. If R^2 = 1.0 indicates a perfect fit which results in a very dependable model for future forecasts, a value of .0 would suggest that the model completely failed to formulate the data.

The Durbin–Watson statistic (DW) was applied to identify whether multicollinearity exists. This statistic can take on values ranging from 0 to 4, with a value of 2 indicating the absence of a correlation between the variables used in its calculation. Consequently, a value between 1.5 and 2.5 is suitable for building multicollinearity-free models. This section discusses mathematical expressions and models.

10.3389/fmats.2022.1052870

TABLE 6 Crack characteristics and mechanical properties with different fibre fractions for mortar mixes.

Mix ID	W/C ratio	Average crack width (mm)	Crack age (days)	Crack area (mm^2)	Tensile strength (MPa) (3 days)	Compressive strength (MPa) (3 days)
PM1	.3	.20	9	15.00	2.95	39.72
M1-V_f 0.4	.3	.14	10	11.70	3.21	40.51
M1-V_f 0.6	.3	.11	12	8.36	3.50	41.25
M1-V_f 0.8	.3	.07	13	2.52	4.40	57.90
PM2	.4	.10	14	7.50	1.13	24.65
M2-V_f 0.4	.4	.04	16	3.536	1.60	32.35
M2-V_f 0.6	.4	.02	17.5	1.28	1.90	37.35
M2-V_f 0.8	.4	.001	18	.012	2.09	39.66
PM3	.5	.055	17.13	3.70	.73	21.35
M3-V_f 0.4	.5	.014	19.33	.845	.93	22.25
M3-V_f 0.6	.5	.007	20.48	.074	1.02	24.90
M3-V_f 0.8	.5	.004	22.50	.02	1.13	24.50

TABLE 7 Crack characteristics and mechanical properties with different fibre fractions for cement-paste mixes.

Mix ID	W/C ratio	Average crack width (mm)	Crack age (h)	Crack Area (mm^2)	Tensile strength (MPa) (3 days)	Compressive strength (MPa) (3 days)
PM4	.3	.506	32	38	1.9	45.8
M4-Vf 0.4	.3	.23	45	22.5	2.5	46.8
M4-Vf 0.6	.3	.14	48	10.65	2.8	47
M4-Vf 0.8	.3	.11	56	4.05	3.2	48.1
PM5	.4	0.4	60	30	1.7	34.9
M5-Vf 0.4	.4	.17	72	15	1.9	35.7
M5-Vf 0.6	.4	0.1	74	6.45	2.1	38.7
M5-Vf 0.8	.4	.07	79	.835	2.5	38
PM6	.5	0.3	68	19.35	1.1	25.2
M6-Vf 0.4	.5	.15	75	9.175	1.2	26.3
M6-Vf 0.6	.5	.09	79	.945	1.5	27
M6-Vf 0.8	.5	.03	92	.150	1.45	27.3

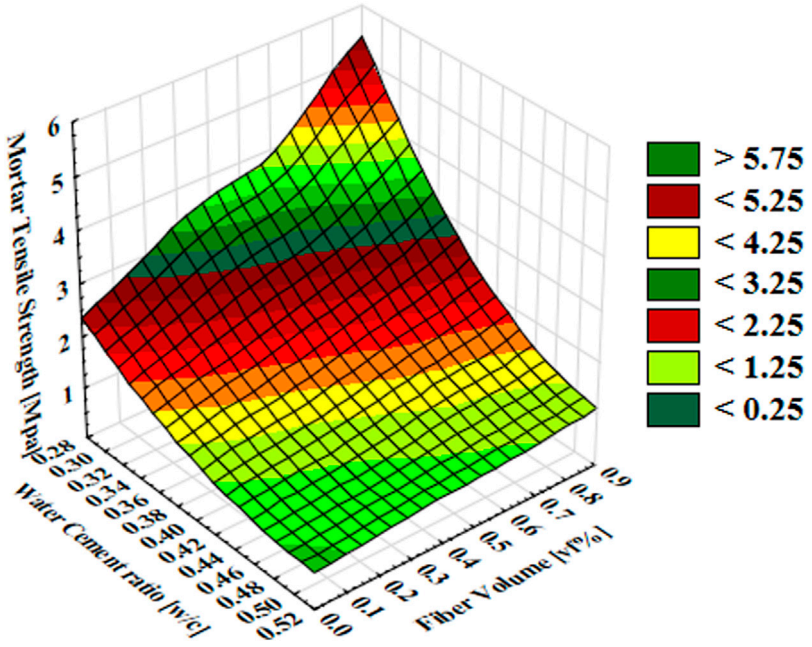

FIGURE 4
Mortar tensile strength, MPa against fibre-volume fraction, V_f (%) and water-cement (w/c) ratio.

$$DW = \frac{\sum_{t=2}^{T}(e_t - e_{t-1})}{\sum_{t=1}^{T} e_t^2}$$

where DW is the Durbin–Watson test, while e_t and e_{t-1} represent the least-squares regression residuals.

3 Results and discussion

The mechanical and early-age cracking performances of fibre-cement paste and mortar are strongly dependent on the w/c ratio and dosage of fibre. This study focused on how the mechanical properties and early-age cracking shrinkage are influenced by the fibre V_f and its corresponding w/c ratio. The test results for the crack characteristics and mechanical properties with different fibre fractions for different mortar mixes are listed in Table 6.

The test results for the crack characteristics and mechanical properties with different fibre fractions for different cement-paste mixes are listed in Table 7.

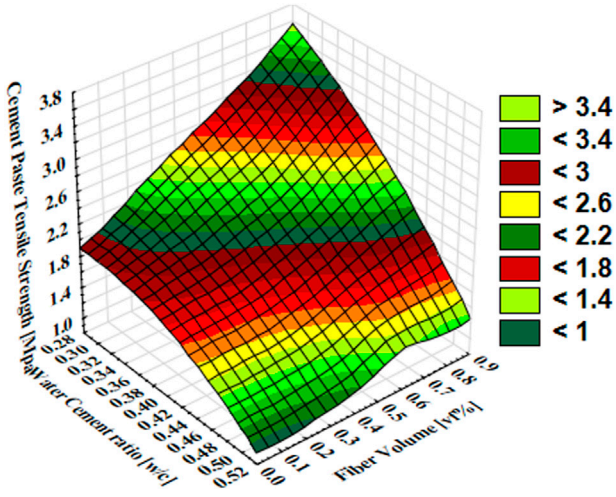

FIGURE 5
Cement-paste tensile strength (MPa) against the fibre-volume fraction, V_f (%) and water-cement (w/c) ratio.

3.1 Tensile strength

Results given in Table 6 show that the tensile strength increases as PP increases at a specific water-cement ratio and decreases as the water-cement ratio increases. The tensile strength of the mortar with PP fibres increased from 2.95 to 4.4 MPa as the fibre dosage increased from 0% to .8%, where the water-cement ratio was .3. When the ratio of water to cement was .4 and .5, the tensile strength increased from 1.13 to 2.09 MPa and from .029 to .75 MPa as the fibre dosage increased from 0% to .8% V_f, respectively. These results are in good agreement with previously published research studies (Wu et al., 2020; Yan et al., 2021). Figure 4 presents the effects on the tensile strength when adding fibre with different water-to-cement ratios for different mortar mixes. Figure 4 is plotted using distance-weighted least squares.

In Figure 4, a significant effect can be seen when adding PP to the mortar. When adding .4% more V_f, the increase ranged from 26% to 53% when the ratio of water-cement ratio varied from .3 to .5. When

TABLE 8 Proposed tensile-strength equations for mortar and cement paste against PP, V_f, and w/c ranging from .3 to .5

Mix group	Equation	R^2	DW
Mortar	$T_{sm} = 5.934 + 1.472V_f - 11.583\ (w/c)$	.894	1.901
Cement paste	$T_{scp} = 4.105 + 1.017V_f - 6.437\ (w/c)$	.936	1.131

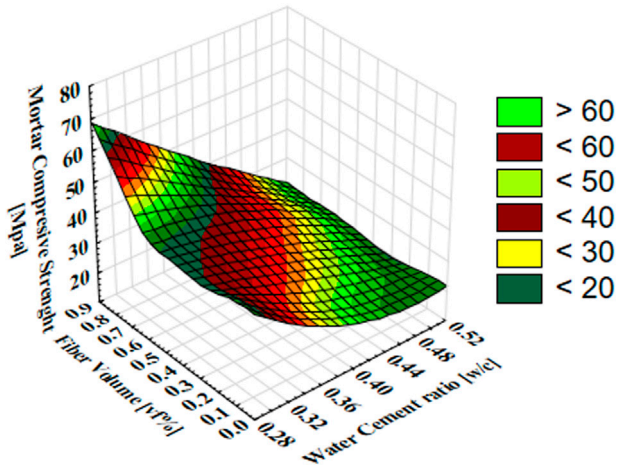

FIGURE 6
Mortar compressive strength (MPa) against fibre V_f and water-cement (w/c) ratio.

adding .8% more V_f, the increase ranged from 54% to 110% as the water-cement ratio decreased from .5 to .3, respectively.

Figure 5 presents the effects on tensile strength when adding fibre with different water-to-cement ratios for different cement-paste mixes. In Figure 5, a significant effect of adding PP fibre to the cement paste can be evaluated. When adding .4% more V_f, the increase ranged from 9% to 32% when the ratio of water to cement went from .5 to .3. When adding .8% more V_f, the increase ranged from 32% to 68% when the ratio of water to cement decreased from .5 to .3, respectively. The magnitude of the tensile strength was highly predictive of the crack severity. However, it is evident that the advantage of fibres is not limited to their capacity to reduce the shrinking strain. The effectiveness of the fibres is attributable, at least in part, to their capacity to bridge cracks and restrict their growth.

Table 8 presents the relevant equations for the tensile strength against the PP fibre V_f (%) and water-cement ratio for the mortar and cement-paste mixes. The values of R^2 present a high correlation. The DW indicates no collinearity for the tensile strengths of mortar mixes, while the cement paste DW indicates minor collinearity. These equations are limited to being used for tensile-strength response predictions of mortars and cement pastes with polypropylene fibre ($V_f \leq .8\%$) at a w/c ratio range from .3 to .5 in the eccentric-ring test.

The tensile strength increased per unit rise in PP V_f (%) was 1.472 MPa for mortar and 1.017 MPa for cement pastes. The reduction in tensile strength when the w/c ratio was increased was 11.583 MPa for mortar and 6.437 MPa for cement pastes. Thus, increasing the amount of PP fibre will provide better tensile strength, while an increase in associated w/c will weaken this enhancement.

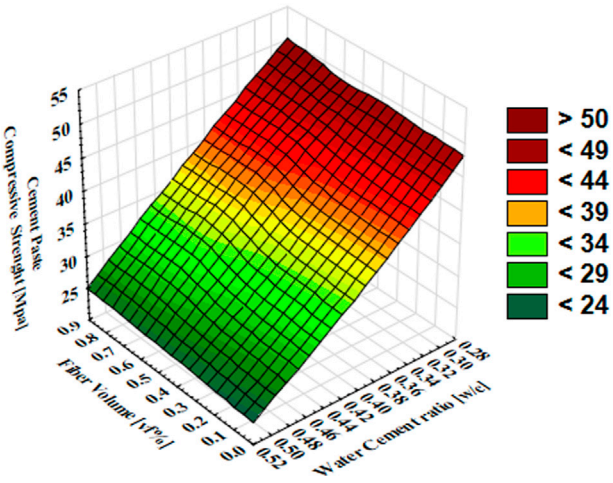

FIGURE 7
Cement-paste compressive strength against fibre V_f and w/c ratio.

3.2 Compressive strength

The results of the compressive strength are shown in Figure 6. The interaction between PP fibre content and the related concrete compressive strength relative to the control sample is demonstrated.

Comparison of the mixes with V_f values of .4%, .6%, and .8% showed that increasing the PP fibre enhanced the compressive strength. The rate of increase indicates a continuing upward trend in compressive strength that varies with the w/c ratio. The compressive strength of the mortar with PP fibres increases from 39.72 to 57.9 MPa (45.8%) as the fibre V_f increases from 0% to .8%, where the w/c ratio was .3. When the ratio of w/c was .4 and .5, the compressive strength increased from 24.62 to 39.66 MPa (61%) and 21.3–24.46 MPa (15%), respectively. The highest enhancement in compressive strength was associated with a lower w/c ratio of .3 with a high fibre V_f of .8%. In addition, the compressive strength increased in terms of cement-to-sand 1:2 mixtures with a w/c ratio of .4. The results agree well with the findings of a previous study (Yuan and Jia, 2021).

Figure 7 demonstrates the relationship between compressive strength (MPa) against fibre V_f and w/c ratio for the cement-paste mixes.

When fibres were added to mixes to increase their strength, there was no weighty variation in compressive strength (5% increase) with a w/c ratio of .3 and V_f of .8%. When the w/c ratio was .4 and .5 with a V_f of .8%, the compressive strength increased by 9.0% and 8.3%, respectively. This is in line with other studies (Wu et al., 2020). Thus, adding PP fibres to cement pastes is insufficient to significantly affect the compressive strength. This is because the strength of concrete is determined by the bond between cement and fine or coarse aggregates.

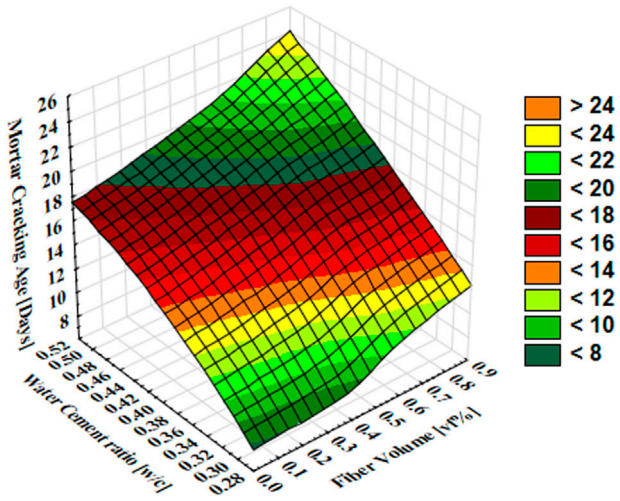

FIGURE 8
Mortar-cracking age (days) against fibre V_f (%) and w/c ratio.

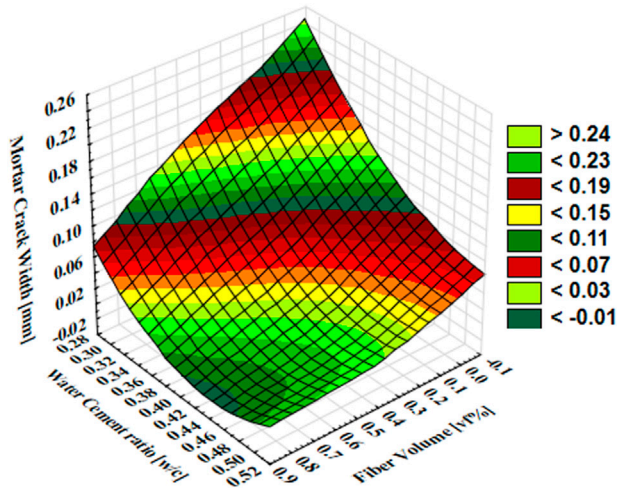

FIGURE 10
Mortar-crack width against fibre V_f and w/c ratio.

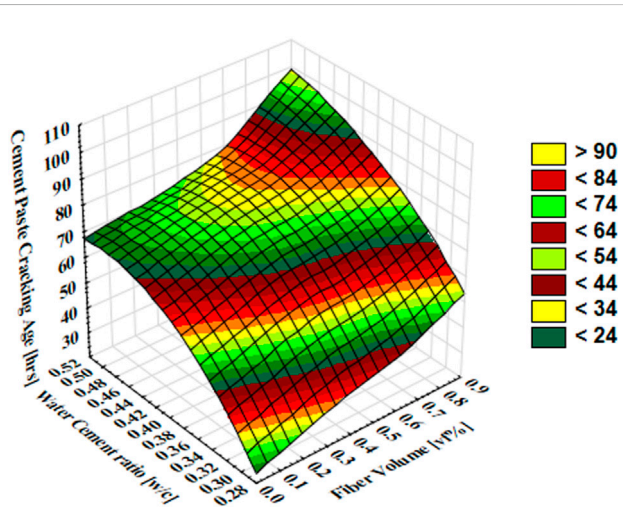

FIGURE 9
Cement-paste cracking age (h) against fibre V_f (%) and w/c ratio.

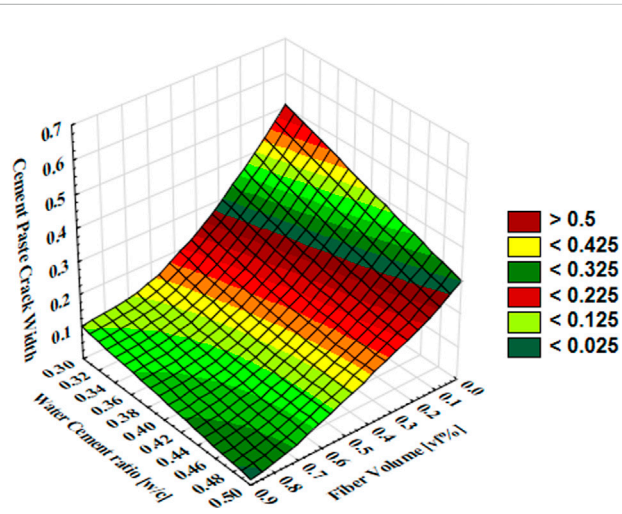

FIGURE 11
Cement-paste crack width against fibre V_f and w/c ratio.

3.3 Restrained-shrinkage cracking test

3.3.1 Crack age

The reduction in the stress development rate when the w/c ratio rises delays its cracking age. This confirms the higher crack tendency of the lower w/c ratio mixes, which is consistent with literature (Bentur and Kovler, 2003; Tian and Wei, 2019). Adding fibre to the mixtures strengthened them and delayed the appearance of cracks, as shown in Figures 8, 9 below. The crack age was detected and recorded as soon as the crack appeared on the surface of each specimen. For mortar mixtures with a low w/c ratio of .3, the cracking age was 9 days for the plain mixture (PM1). Adding .4%, .6%, and .8% V_f of PP fibres delayed the crack age by 10, 12, and 13 days, respectively. As shown in Figure 8, adding fibres delayed the crack age from 14 to 18 days and 20–23 days by adding a high Vf of .8% to PM2 and PM3, respectively.

Identical results were obtained with cement-paste mixtures with .4 and .5 w/c ratios, as shown in Figure 9. Cement-paste mixtures were labelled and a w/c ratio of .3 was considered low. The first crack appeared after 32 h for the PM4. The existence of cracks propagated three to four times longer in fibre-reinforced mixes than in unreinforced mixtures. The PP dispersion fibres were the most advantageous due to their higher surface area, which results in greater frictional restraint, and their ability to bridge cracks due to the increased number of regularly spaced filaments.

3.3.2 Crack width

The results of the crack width are given in Tables 6, 7 for the mortar and cement-paste mixes, respectively. Figure 10 shows the relationship between the mortar-crack width and fibre V_f (%) and w/c ratio. Compared with plain mixtures, the crack width was reduced by 99.9% for 1:2 mix proportions by adding a V_f of .8% with a w/c ratio of .4. For a w/c ratio of .5, the cracking width was reduced by 74%–92%.

TABLE 9 Comparison between cement-paste cracking width and mortar cracking width with equal w/c ratios.

W/c ratio = .4	M2: Cement-paste cracking width (mm)				M5: Mortar cracking width (mm)			
	P.M.	.4% V_f	.6% V_f	.8% V_f	P.M.	.4% V_f	.6% V_f	.8% V_f
Crack width	.4	.17	0.1	.07	0.1	.04	.02	.001
CRR	0%	58%	75%	83%	0%	60%	80%	99%

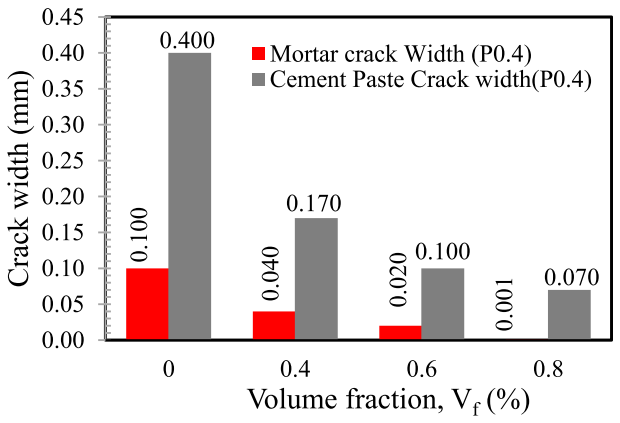

FIGURE 12
Histogram plot of crack width and fibre V_f for cement paste and mortar.

The PP fibres completely decreased shrinkage cracking. The amount of fine aggregate was reduced in 1:1 mix proportions with a low w/c ratio of .3 as the volume of cement and water was increased; consequently, more strain shrinkage and cracking occurred. These results agree with those of previous studies (Alavi Nia et al., 2012).

The CRR (cracking reduction ratio) was calculated using the following equation (CWpp/CWnpp: maximum crack width of fiber mortar mixture/control mortar mixture):

TABLE 10 Proposed equation of crack width of mortar and cement paste with PP and w/c ranging from .3 to .5 in the eccentric-ring test.

Mix group	Model	R^2	DW
Mortar	CWR_m = .572–1.525 (w/c)—1.102V_f	.921	1.92
Cement paste	CWR_{cp} = -.02–.061 (w/c)—1.069V_f	.962	1.945

$$CRR = 100 \times \left(1 - CW_{pp}/CW_{npp}\right)$$

Where

CW_{pp}: maximum crack width of fiber mortar mixture

CWnpp/: control mortar mixture.

Here, the effect of fibres with different V_f values might be more clearly identified. Figure 10 shows the effect of the fibre on decreasing the crack width by 60%–99% when V_f changes from .4% to .8%.

Figure 11 shows the relationship between the cement-paste crack width, fibre V_f, and w/c ratio. For cement-paste mixtures with a V_f of .4%–.8%, crack widths were reduced by 55%–78%, 58%–83%, and 50%–90% for w/c ratios of .3, .4, and .5, respectively. The plain control cement failed to meet these criteria. However, after the fibres were added, the requirements were satisfied. Hence, fibres can function as crack bridges, preventing shrinkage cracking. Table 9 shows a comparison between the cement-paste and mortar cracking widths with equal w/c ratios.

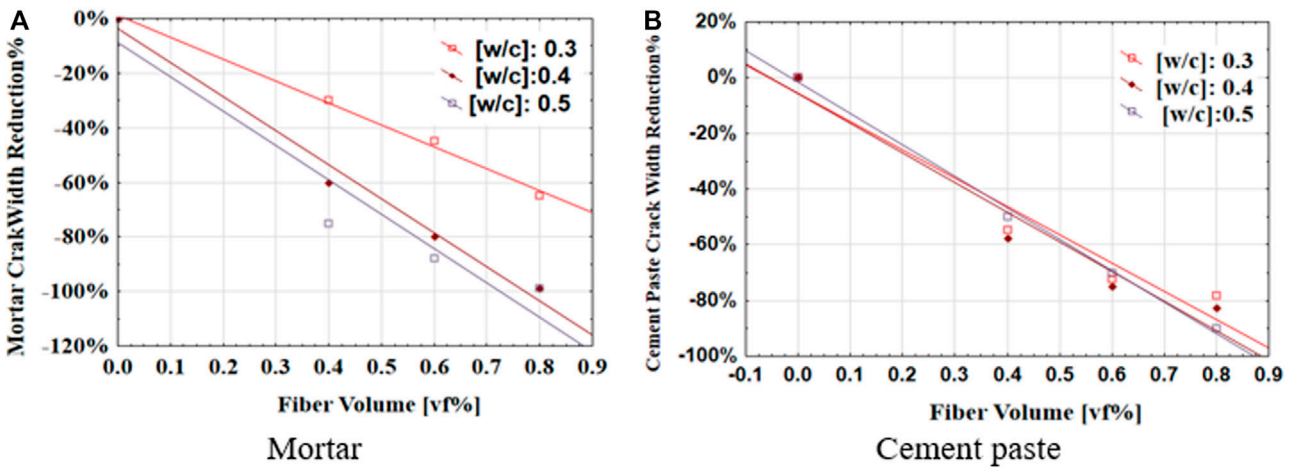

FIGURE 13
Crack-width reduction percentage at different w/c with different fibre V_f for **(A)** Mortar and **(B)** Cement paste.

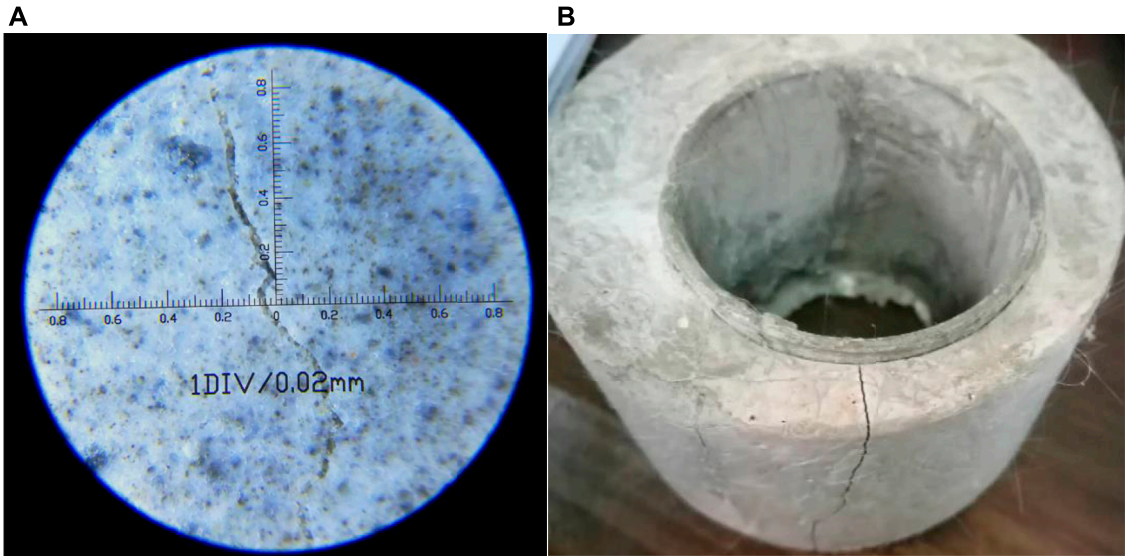

FIGURE 14
(A) Microcrack width measurement and **(B)** Crack sample using the eccentric-ring test.

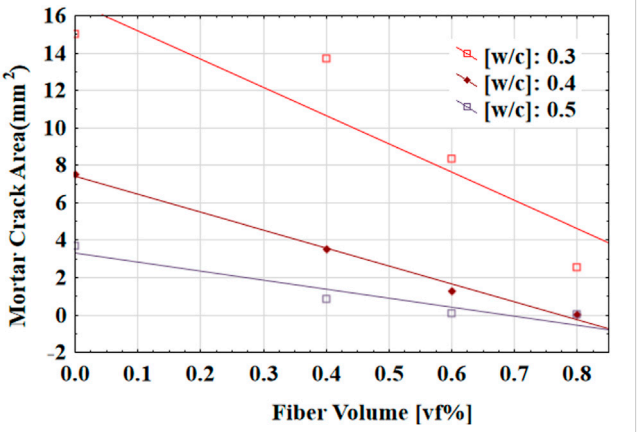

FIGURE 15
Mortar-crack area against fibre V_f.

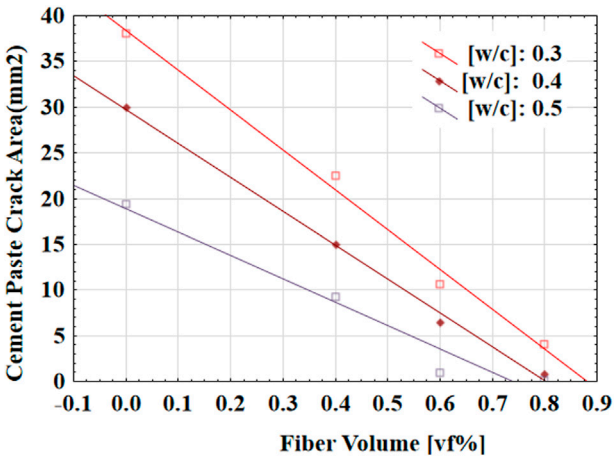

FIGURE 16
Cement-paste crack area against fibre V_f.

As shown in Table 9 and Figure 12, adding fine aggregates can strengthen the mixtures by reducing the amount of cement and water. The cement paste M2 and mortar M5 had the same w/c ratio of .4 and equal Vf dosages (.4–.08%). The amount of M5 fine aggregate increased the unit volume of cement and water. Since the shrinkage is largely influenced by the pore water pressure of evaporating water, this resulted in greater shrinkage strain and more cracking.

Figure 12 illustrates the cement-paste and mortar-crack widths for different fibre V_f.

Table 10 presents the relevant equations for reducing the crack widths resulting from the addition of V_f (%) and w/c ratio for all mortars and cement pastes. The R^2 values indicate a significant correlation, whereas the Durbin–Watson [DW] values show that these models are free from collinearity. These equations are limited to being used for prediction of the response of the crack width of mortars and cement paste with polypropylene fibre ($V_f \leq .8\%$) at a w/c ratio range from .3 to .5 in the eccentric-ring test. Figure 13 illustrates the reduction in crack-width percentage at different w/c ratios and fibre V_f for the mortar and cement paste.

The increase in crack width per unit of fibre-volume fraction V_f was reduced by 1.102% for mortar and 1.017% for cement-paste mixes. The reduction rate of crack width when the w/c ratio was increased was 1.525% for mortar, whereas it was only .061% for cement-paste mixes. As a result, increasing the amount of PP fibres would result in a better reduction in crack width, while any decrease in the associated w/c would mitigate this reduction.

3.3.3 Crack area

Figures 14A, B show the microcrack width measurement using a 100-magnification microscope and crack sample using an eccentric-ring test, respectively. Another metric used to evaluate the extent of cracking through the ring is the measurement of the cracking area. To calculate the cracking area of a ring sample, the length and breadth of all cracks were measured using a microscope with a 100-magnification. The areas of all cracks were added together.

Figure 15 illustrates the relationship between the crack area and fibre V_f for mortar mixes with different w/c ratios.

The scattering PP fibres reduced the cracking area for a w/c ratio of .3 by approximately 22%, 44.3%, and 83.2% for V_f values of .4%, .6%, and .8%, respectively. Contrarily, adding PP fibres reduced the cracking area by 52.8%, 82.9%, and 99.8% with .4%, .6%, and .8%, respectively for a .4 w/c ratio. The mixtures with a .5 w/c ratio demonstrated the capability of the PP fibres to limit crack growth. The reduction percentages were 77.2%, 98%, and 99.5% with V_f values of .4%, .6%, and .8%, respectively.

Figure 16 shows the relationship between the crack area and fibre (V_f) for the cement-paste mixes with different w/c ratios.

The addition of PP fibres to the cement paste significantly reduced the cracking area. When V_f was .2%, the crack area decreased by 40.8%, 50.6%, and 52.6% with w/c ratios of .3, .4, and .5, respectively. When the PP fibre content was .4, the reduction increased noticeably to 72.1%, 78.5%, and 95.1%. The reduction slowed when V_f was .8, reaching 99.2% at a w/c ratio of .5.

4 Conclusion

The results of this study can be summarised as follows:

1. The eccentric-ring approach more instantly reflects the cracking time, position, and other cracking parameters of the cement-mortar composites. This demonstrates how a material cracks, and the best way to study the cracking properties of fibrous mixtures is to determine how the fibres affect the crack properties.
2. This study is useful for discovering the behaviour of both restrained cement paste and mortar regarding cracking width, age, and area, and for using less prone-to-crack concrete combinations.
3. The addition of PP fibres with different V_f values to mortar and cement pastes has a substantial impact on the tensile strength. The effect of fibre dosage on V_f was estimated for different w/c ratios. The increases in tensile strength were 26%–110% and 9%–68% in the mortar and cement paste, respectively. The higher the V_f and lower the w/c ratio, the higher the tensile-strength improvement percentage.
4. Increasing the w/c ratio and amount of fine aggregates increased the cracking age.
5. Formulas for estimating the tensile strength and crack width based on the PP fibre V_f with different w/c ratios of .3–.5 were proposed. The rate of enhancement of the tensile strength or percentage of crack-width reduction was estimated.

Data availability statement

The original contributions presented in the study are included in the article/Supplementary Material, further inquiries can be directed to the corresponding authors.

Author contributions

Conceptualization and design of the research, MA; methodology, MA; formal analysis, MA, MB, and ZM; investigation, MA; resources, ZM; data curation, MA and MB; writing—original draft preparation, MA and MB; writing—review and editing, ZM and MB; visualization, MA and ZM; supervision MB and ZM; project administration, ZM and MH; funding acquisition, ZM and MH.

Conflict of interest

The authors declare that the research was conducted in the absence of any commercial or financial relationships that could be construed as a potential conflict of interest.

Publisher's note

References

Abusogi, M. A., and Bakri, M. (2022). Behaviour of cementitious composites reinforced with polypropylene fibres using restrained eccentric ring test. *Case Stud. Constr. Mater.* 16, e00841. doi:10.1016/j.cscm.2021.e00841

Abusogi, M. A., and Wei, X. (2018). Experimental and numerical analysis of restrained early age cracking based on electrical resistivity using eccentric sample. *J. Wuhan Univ. Technol. Mater. Sci. Ed.* 33, 1472–1480. doi:10.1007/s11595-018-1993-7

Abusogi, M. A., and Wei, X. S. (2019). Numerical analysis to evaluate the effect of restrained edge distance on early age cracking due to drying shrinkage. *Int. J. GEOMATE* 17, 281–287. doi:10.21660/2019.63.08499

Abusogi, M. A., Xiaosheng, W. E. I., and lei, F. (2017). Using eccentrically sample to find the relationship between resistivity and cracking time in cement paste vides mechanical strength and electrical resistivity. *Am. J. Civ. Eng. Archit.* 5, 154–159. doi:10.12691/ajcea-5-4-3

Alavi Nia, A., Hedayatian, M., Nili, M., and Sabet, V. A. (2012). An experimental and numerical study on how steel and polypropylene fibers affect the impact resistance in fiber-reinforced concrete. *Int. J. Impact Eng.* 46, 62–73. doi:10.1016/j.ijimpeng.2012.01.009

Banthia, N., Azzabi, M., and Pigeon, M. (1993). Restrained shrinkage cracking in fibre-reinforced cementitious composites. *Mater. Struct.* 26, 405–413. doi:10.1007/BF02472941

Banthia, N., and Gupta, R. (2006). Influence of polypropylene fiber geometry on plastic shrinkage cracking in concrete. *Cem. Concr. Res.* 36, 1263–1267. doi:10.1016/j.cemconres.2006.01.010

Bentur, A., and Kovler, K. (2003). Evaluation of early age cracking characteristics in cementitious systems. *Mater. Struct.* 36, 183–190. doi:10.1617/14014

Boghossian, E., and Wegner, L. D. (2008). Use of flax fibres to reduce plastic shrinkage cracking in concrete. *Cem. Concr. Compos.* 30, 929–937. doi:10.1016/j.cemconcomp.2008.09.003

Branston, J., Das, S., Kenno, S. Y., and Taylor, C. (2016). Influence of basalt fibres on free and restrained plastic shrinkage. *Cem. Concr. Compos.* 74, 182–190. doi:10.1016/j.cemconcomp.2016.10.004

C109/C109M-16a, A. (2016). *Standard test method for compressive strength of hydraulic cement mortars (using 2-in. or [50-mm] cube specimens)*. West Conshohocken: ASTM International.

Choktaweekarn, P., and Tangtermsirikul, S. (2009). A model for predicting coefficient of thermal expansion of cementitious paste. *ScienceAsia* 35, 57–63. doi:10.2306/scienceasia1513-1874.2009.35.057

Dahish, H. A., Bakri, M., and Alfawzan, M. S. (2021). Predicting the strength of cement mortars containing natural pozzolan and silica fume using multivariate regression analysis. *Int. J. GEOMATE* 20, 68–76. doi:10.21660/2021.82.j2021

Dalvand, A., and Ahmadi, M. (2021). Impact failure mechanism and mechanical characteristics of steel fiber reinforced self-compacting cementitious composites containing silica fume. *Eng. Sci. Technol. Int. J.* 24, 736–748. doi:10.1016/j.jestch.2020.12.016

Dong, W., Yuan, W., Zhou, X., and Wang, F. (2018). The fracture mechanism of circular/elliptical concrete rings under restrained shrinkage and drying from top and bottom surfaces. *Eng. Fract. Mech.* 189, 148–163. doi:10.1016/j.engfracmech.2017.10.026

Dong, W., Zhou, X., and Wu, Z. (2014). A fracture mechanics-based method for prediction of cracking of circular and elliptical concrete rings under restrained shrinkage. *Eng. Fract. Mech.* 131, 687–701. doi:10.1016/j.engfracmech.2014.10.015

Dong, W., Zhou, X., Wu, Z., and Xu, B. (2017). Investigating crack initiation and propagation of concrete in restrained shrinkage circular/elliptical ring test. *Mater. Structures/Materiaux Constr.* 50, 73–13. doi:10.1617/s11527-016-0942-1

Hossain, A. B., and Weiss, J. (2006). The role of specimen geometry and boundary conditions on stress development and cracking in the restrained ring test. *Cem. Concr. Res.* 36, 189–199. doi:10.1016/j.cemconres.2004.06.043

Idrees, M., Akbar, A., Saeed, F., Saleem, H., Hussian, T., and Vatin, N. I. (2022). Improvement in durability and mechanical performance of concrete exposed to aggressive environments by using polymer. *Mater. (Basel)* 15, 3751. doi:10.3390/ma15113751

Juarez, C. A., Fajardo, G., Monroy, S., Duran-Herrera, A., Valdez, P., and Magniont, C. (2015). Comparative study between natural and PVA fibers to reduce plastic shrinkage cracking in cement-based composite. *Constr. Build. Mater.* 91, 164–170. doi:10.1016/j.conbuildmat.2015.05.028

Kanavaris, F., Azenha, M., Soutsos, M., and Kovler, K. (2019). Assessment of behaviour and cracking susceptibility of cementitious systems under restrained conditions through ring tests: A critical review. *Cem. Concr. Compos.* 95, 137–153. doi:10.1016/j.cemconcomp.2018.10.016

Lye, C.-Q., Dhir, R. K., and Ghataora, G. S. (2022). Estimation models for creep and shrinkage of concrete made with natural, recycled and secondary aggregates. *Mag. Concr. Res.* 74, 392–418. doi:10.1680/jmacr.20.00007

McLain, D. H. (1974). Drawing contours from arbitrary data points. *Comput. J.* 17, 318–324. doi:10.1093/comjnl/17.4.318

Rani, S. Y., Nusari, M. S., bin Non, J., Poddar, S., and Bhaumik, A. (2022). Durability of geopolymer concrete with addition of polypropylene fibre. *Mater. Today Proc.* 56, 2846–2851. doi:10.1016/j.matpr.2021.10.164

Rezaie, Y., Sharifi, S. M. H., and Rashed, G. R. (2022). Probabilistic fracture assessment of snake laid pipelines under high pressure/high temperature conditions by engineering critical assessment. *Eng. Fract. Mech.* 271, 108592. doi:10.1016/j.engfracmech.2022.108592

Sadiqul Islam, G. M., and Gupta, S. Das (2016). Evaluating plastic shrinkage and permeability of polypropylene fiber reinforced concrete. *Int. J. Sustain. Built Environ.* 5, 345–354. doi:10.1016/j.ijsbe.2016.05.007

Saradar, A., Tahmouresi, B., Mohseni, E., and Shadmani, A. (2018). Restrained shrinkage cracking of fiber-reinforced high-strength concrete. *Fibers* 6, 12. doi:10.3390/fib6010012

Tang, J., Swolfs, Y., Yang, M., Michielsen, K., Ivens, J., Lomov, S. V., et al. (2018). Discontinuities as a way to influence the failure mechanisms and tensile performance of hybrid carbon fiber/self-reinforced polypropylene composites. *Compos. Part A Appl. Sci. Manuf.* 107, 354–364.

Tian, C., and Wei, X. (2019). Early shrinkage cracking of cementitious materials based on the eccentric ring method. *Constr. Build. Mater.* 216, 599–611. doi:10.1016/j.conbuildmat.2019.05.014

Wongtanakitcharoen, T., and Naaman, A. E. (2007). Unrestrained early age shrinkage of concrete with polypropylene, PVA, and carbon fibers. *Mater. Structures/Materiaux Constr.* 40, 289–300. doi:10.1617/s11527-006-9106-z

Wu, H., Lin, X., and Zhou, A. (2020). A review of mechanical properties of fibre reinforced concrete at elevated temperatures. *Cem. Concr. Res.* 135, 106117. doi:10.1016/j.cemconres.2020.106117

Xu, Y., Xing, G., Zhao, J., and Zhang, Y. (2021). The effect of polypropylene fiber with different length and dosage on the performance of alkali-activated slag mortar. *Constr. Build. Mater.* 307, 124978. doi:10.1016/j.conbuildmat.2021.124978

Yan, P., Chen, B., Afgan, S., Aminul Haque, M., Wu, M., and Han, J. (2021). Experimental research on ductility enhancement of ultra-high performance concrete incorporation with basalt fibre, polypropylene fibre and glass fibre. *Constr. Build. Mater.* 279, 122489. doi:10.1016/j.conbuildmat.2021.122489

Yousefieh, N., Joshaghani, A., Hajibandeh, E., and Shekarchi, M. (2017). Influence of fibers on drying shrinkage in restrained concrete. *Constr. Build. Mater.* 148, 833–845. doi:10.1016/j.conbuildmat.2017.05.093

Yuan, Z., and Jia, Y. (2021). Mechanical properties and microstructure of glass fiber and polypropylene fiber reinforced concrete: An experimental study. *Constr. Build. Mater.* 266, 121048. doi:10.1016/j.conbuildmat.2020.121048

Zhang, G., Song, J., Yang, J., and Liu, X. (2006). Performance of mortar and concrete made with a fine aggregate of desert sand. *Build. Environ.* 41, 1478–1481. doi:10.1016/j.buildenv.2005.05.033

Zhang, W., Lin, H., Xue, M., Wang, S., Ran, J., Su, F., et al. (2022). Influence of shrinkage reducing admixtures on the performance of cementitious composites: A review. *Constr. Build. Mater.* 325, 126579. doi:10.1016/j.conbuildmat.2022.126579

Zhou, X., Ph, D., Asce, M., Dong, W., Ph, D., and Oladiran, O. (2014). Experimental and numerical assessment of restrained shrinkage cracking of concrete using elliptical ring specimens. doi:10.1061/(ASCE)MT.1943-5533